Chemical Sputtering of Carbon Materials due to Combined Bombardment by Ions and Atomic Hydrogen

W. Jacob*, C. Hopf, and M. Schlüter
Max-Planck-Institut für Plasmaphysik, EURATOM Association, Boltzmannstr. 2, 85748 Garching, Germany

Simultaneous interaction of low-energy ions and atomic hydrogen—a process named chemical sputtering—causes erosion of C:H surfaces which is significantly higher than the sum of the individual processes—chemical erosion due to atomic hydrogen alone and physical sputtering due to ions. Above that, this process occurs also at energies below the threshold for physical sputtering. A microscopic reaction mechanism for chemical sputtering was recently suggested. A mathematical model based on this reaction mechanism is able to quantitatively reproduce the energy dependence of chemical sputtering by atomic hydrogen and argon using just one free parameter. The model is briefly reviewed and the underlying physical processes are discussed. We present new predictions for the chemical sputtering of carbon by atomic hydrogen and different ions relevant to plasma–wall interaction in nuclear fusion devices (He^+, H^+, D^+, T^+, and Ne^+) and new experimental data for the chemical sputtering due to hydrogen and Ne^+ ions.

PACS numbers: 79.20.Rf, 82.65.+r, 81.65.Cf, 52.40.Hf
Published with Physica Scripta: Received 25 April 2005
Accepted for publication 29 June 2005
Published 26 April 2006
Physica Scripta **T124** (2006) 32–36

I. INTRODUCTION

For the time being, one of the most crucial plasma–wall-interaction issues for a next-step device such as ITER is tritium retention. The actual ITER design uses beryllium for the main chamber wall and carbon as well as tungsten in the divertor [1]. For this choice of materials, tritium co-deposition with eroded carbon is expected to be the dominant tritium retention mechanism. This holds even for the planned scenario that only a small fraction of the total wall area, more precisely the divertor strike zones, are made of carbon [1].

The process of tritium retention in redeposited layers can roughly be separated into three steps: (i) erosion, (ii) transport through the boundary plasma, and (iii) surface reactions of neutral carbon carrying species at remote surface areas. This paper deals with the first step, the erosion process which leads to the production of volatile hydrocarbon species through interaction of the plasma species with carbon surfaces. The most important plasma species in this context are energetic particles (ions and neutrals) and hydrogen atoms.

It is well known from a large number of experimental investigations that the combined interaction of atomic hydrogen and energetic ions or the sputtering with hydrogen ions leads to enhanced sputtering yields (see e.g. [2] and references therein, [3, 4]). This process is often referred to as *'chemical erosion'*, but this name may be misleading because it is also used for the thermally activated chemical erosion due to atomic hydrogen alone.

Recently, Hopf *et al.* [5, 6] investigated the combined interaction of argon ions and H atoms with plasma-deposited hydrocarbon layers in the low-energy region (20–800 eV). Like other researchers before [2], they found a significantly enhanced erosion yield compared with the sum of the individual processes—physical sputtering due to ion bombardment and chemical erosion due to hydrogen atoms. Erosion due to the combined interaction of reactive neutrals and energetic ions was named *chemical sputtering* according to the definition given by Winters and Coburn [7]. Based on a microscopic model Hopf *et al.* devised a framework for understanding chemical sputtering of carbonaceous surfaces which allows for a quantitative description of the observed energy dependence [6]. This paper presents new data using Ne^+ ions and an extrapolation of the model to other ion species relevant to the plasma–surface interaction in nuclear fusion devices such as He^+, H^+, D^+, and T^+.

II. EXPERIMENTAL

Experiments were carried out in the MAJESTIX device at IPP Garching. A detailed description of the experimental setup and applied techniques is presented in Ref. [8]. In short: MAJESTIX is an ultra-high-vacuum-based particle-beam experiment to study heterogeneous surface reactions relevant to plasma–surface interaction processes. The experiment comprises two radical beam sources and a source for low energy ions. Erosion rates are determined using real-time *in situ* ellipsometry. The fluxes of the radical beam sources are absolutely quantified for the production of hydrogen atoms and methyl radicals. The ion source allows to produce quantified ion beams for a wide variety of ionic species, e.g. He^+, Ne^+, Ar^+, H^+, H_2^+, and H_3^+. Ion energies from above 1 keV down to below 10 eV are achievable. The setup allows us to investigate heterogeneous surface processes of one single species or the simultaneous interaction of up to three different, individually controllable species with a surface of interest. Running

*Email address: Wolfgang.Jacob@ipp.mpg.de

the radical sources to produce hydrogen and methyl radicals and the ion source with the mentioned ions, microscopic surface processes relevant for deposition and erosion of hydrocarbon layers in low-pressure gas discharges can be studied in great detail [9]. In the experiments described in this paper only two sources are used, the ion source and one radical source to produce atomic hydrogen.

III. RESULTS AND DISCUSSION

A. Chemical sputtering due to combined exposure to Ar ions and atomic H

Recently, Hopf *et al.* [5, 6] investigated erosion of amorphous hydrogenated carbon (a-C:H) films due to combined Ar^+ ion and thermal atomic hydrogen atom impact. A hard a-C:H film was exposed to either one of the beams alone or to the combined Ar^+ ion and H atom beams. The resulting erosion rates were measured *in situ* by real-time ellipsometry. The corresponding erosion yields were calculated by normalizing the measured rates to the ion flux density which was between 3×10^{12} and $4 \times 10^{12}\,\mathrm{cm^{-2}\,s^{-1}}$. The hydrogen atom flux density was $\sim 1.4 \times 10^{15}\,\mathrm{cm^{-2}\,s^{-1}}$. The experiments were performed at a surface temperature of about 340 K for technical reasons (see [8]).

Figure 1 shows the erosion yield as a function of ion energy. As all experiments involving ions were performed at approximately constant ion flux density, the yields on the left-hand scale correspond roughly to the rates given on the right-hand scale. The squares show the erosion by ions only. Physical sputtering is observed at energies of 200 eV and above. Below these energies the resulting rates are too low to be reliably detected in the experiment. For comparison, Monte Carlo calculations were performed with the computer code TRIM.SP [10] for a C:H film with an $H/(H+C)$ ratio of 0.3 using a surface binding energy of $E_{sb} = 2.8$ eV. This value was found to describe physical sputtering of our films with Ar^+ [5, 6], Ne^+, He^+ [11], and N_2^+ [12] ions very well. In an earlier publication [6], we used a surface binding energy of $E_{sb} = 4.5\,\mathrm{eV}$—a typical value used to model the physical sputtering of technical graphites [13]. This value reproduces well the energy dependence, but deviates from the data by about a factor of 2. A better agreement with the data is achieved for $E_{sb} = 2.8\,\mathrm{eV}$. The fact that a lower surface binding energy yields a better fit of the data is plausible because we do not sputter a graphite target, but an amorphous hydrogenated carbon layer.

The erosion rate caused by the atomic hydrogen beam alone is shown as dashed line in Fig. 1. Since in the absence of ion bombardment it makes no sense to define an erosion yield (per ion) we cannot compare the erosion yields, but we can compare the erosion rates (right-hand scale). The erosion rate for a hydrogen flux density of $\sim 1.4 \times 10^{15}\,\mathrm{cm^{-2}\,s^{-1}}$ at the substrate temperature of $T = 340\,\mathrm{K}$ is rather small. It is similar to the rate for argon sputtering at 400 eV. For the used H atom flux density, the measured erosion rate of $\sim 9 \times 10^{11}\,\mathrm{cm^{-2}\,s^{-1}}$ results in an erosion yield per H atom (not per ion as the other yields in Fig. 1) of 6.4×10^{-4}. We note that the above erosion rate for the atomic hydrogen flux density is higher than that given in [6]. This is due to a new, more precise determination of the erosion rate and leads to an accordingly higher erosion yield for atomic hydrogen.

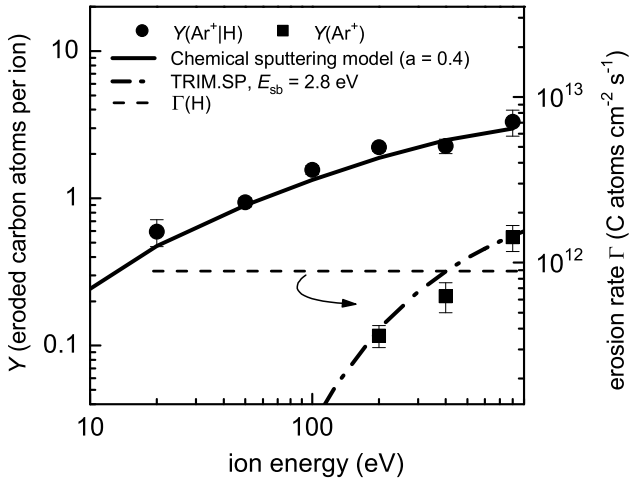

FIG. 1: Energy dependence of the erosion yield $Y(Ar^+)$ of physical sputtering of a C:H film by Ar^+ ions (■) and the yield $Y(Ar^+|H)$ for chemical sputtering by a simultaneous flux of Ar^+ ions and H atoms (•). The dash-dotted line shows the carbon physical sputtering yield as calculated by TRIM.SP [10] for sputtering by argon ions ($E_{sb} = 2.8\,\mathrm{eV}$). The solid line is the result of the chemical sputtering model by Hopf *et al.* [6]. The dashed line shows the absolute erosion rate (right-hand scale) by the applied flux density of H atoms only ($1.4 \times 10^{15}\,\mathrm{cm^{-2}\,s^{-1}}$, atom-to-ion flux ratio ~ 400, $T = 340\,\mathrm{K}$).

If both beams simultaneously interact with the film, the resulting erosion rate greatly exceeds the sum of physical sputtering and thermal chemical erosion; clearly a synergistic mechanism is active—*chemical sputtering*. The chemical sputtering yield decreases with decreasing energy. At the lowest energy being used, 20 eV, the measured rate is, however, still a factor of 2 higher than the rate for pure chemical erosion by the hydrogen flux alone. For the case of simultaneous bombardment (H atoms and Ar^+ ions at 200 eV) the yield per H atom increases from 6.4×10^{-4} (no ions) to 3.5×10^{-3}. In other words, the reactivity of the surfaces towards reaction with atomic hydrogen is increased by a factor of 5.

This general result resembles the findings of erosion experiments applying energetic hydrogen isotopes [2, 14], but in contrast to them a clear decrease of the yield with decreasing ion energy is observed in our case. This difference is most probably due to the fact that we use two separate beams. The physical interaction with the surface is controlled by the impinging noble gas ion beam, while the chemical reactions are determined by atomic hydrogen. Changing the energy of the ion beam we can change the physical interaction while keeping the number and range of chemically reactive species constant. In doing so, we can to a certain extent separate chemical and physical effects. This is not possible in classical ion beam experiments using reactive ion beams [2, 14]. Here chemical and physical effects are interconnected. For example,

the main interaction zone shifts with increasing ion energy to deeper layers while in our experiments the chemical reaction is restricted to the surface-near layer. In fact, the chemical sputtering model can also be extended to the case of reactive ion beams [15]. Further, it should be kept in mind that in our experiment the atomic hydrogen flux density is much higher than the ion flux density.

B. Model for chemical sputtering

Hopf *et al.* [5, 6] proposed the following mechanism for the chemical sputtering of a-C:H: (i) incident ions break C–C bonds within their penetration range leaving behind dangling bonds. (ii) Atomic hydrogen, which is known to penetrate roughly 2 nm into a-C:H [16, 17], passivates the dangling bonds before they recombine otherwise. (iii) Repetition of steps (i) and (ii) finally leads to the formation of volatile hydrocarbons below the surface which diffuse to the surface and desorb. The latter process is thermally driven. The proposed mechanism is also able to explain a couple of findings in the literature as discussed in [6].

Based on this microscopic model of the chemical sputtering mechanism a model was devised which allows to calculate the energy dependence of the $Ar^+|H$ experiment in Fig. 1 (circles) [5, 6]. The chemical sputtering yield is given by the integral over two depth-dependent factors: (i) the yield $y_{bb}(x)\,dx$ at which ions break C–C bonds in an interval dx at a depth x below the surface and (ii) the probability $p_{pass}(x)$ of the passivation of dangling bonds by atomic hydrogen.

The yield $y_{bb}(x,E)$ is determined from TRIM.SP [10] calculations for a given ion energy E counting the number of events where in a binary collision at least an energy E_{bb} is transferred to a carbon atom in the film. E_{bb} is the minimum amount of energy that has to be transferred to a target carbon atom to break a C–C bond. It is chosen within the range of typical C–C bond energies in hydrocarbon molecules as 5 eV. Altogether one obtains

$$Y = a \int y_{bb}^{C}(x) \exp(-x/\lambda)\,dx, \qquad (1)$$

where a is a scaling factor. For $p_{pass}(x)$ we choose an exponential term with a characteristic length of $\lambda = 0.4$ nm (see [5, 6]). The model curve is presented in Fig. 1 as solid line using $a = 0.4$ as scaling factor. Obviously the agreement is very satisfying. With one one free parameter, the model correctly describes the experimentally observed energy dependence.

The dependence on the relative H/ion flux was investigated and discussed by Hopf *et al.* [6]. It was shown that a much higher atomic hydrogen flux density compared with the ion flux density is required to achieve maximal chemical sputtering yields. In the $Ar^+|H$ experiment described in Sect. III A, the ratio of neutral hydrogen to argon ions was 400 [5, 6] and even higher flux ratios are required for saturation of the process.

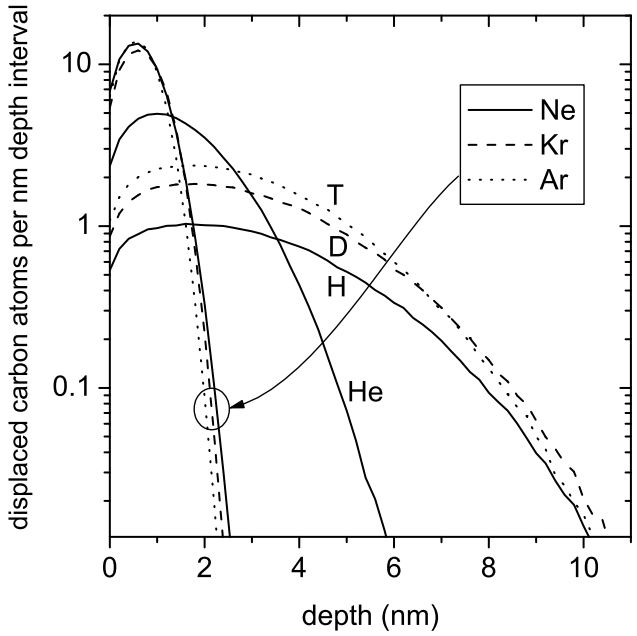

FIG. 2: Depth distributions of the bond-breaking yield y_{bb}^{C} in hard a-C:H ($H/(H+C) = 0.3$) at an energy of 200 eV calculated by TRIM.SP for different projectiles.

C. Model predictions for other ion species

Examples of the depths distributions of the carbon displacement yield y_{bb}^{C} used to calculate the chemical sputtering yield according to Eq. (1) for different atomic ions as projectiles are shown in Fig. 2. Calculations were performed by TRIM.SP [10] for atomic ions impinging on a typical hard a-C:H layer with a hydrogen content of 0.3 ($H/(H+C)$) [18] using a carbon bond-breaking energy $E_{bb}^{C} = 5$ eV. Hydrogen isotopes have the largest range, but a relatively low displacement density (number of displacements per depth interval). At the used energy of 200 eV they penetrate about 10 nm. The range of He ions is about 6 nm, but the displacement density close to the surface is about a factor of 5 higher. The range for Ne ions is about 2.5 nm with an even higher displacement density close to the surface. The depth distributions for Ar and Kr are very similar to those of Ne. If we keep in mind that atomic hydrogen can penetrate only about 2 nm, it is obvious that the different depth distributions presented in Fig. 2 lead to very different chemical sputtering yields.

The interaction of the projectiles with the target atoms is governed by three factors: Firstly and most importantly, the dependence of the scattering cross section on the nuclear charge of the projectile ($\sim Z^2$ for simple Coulomb scattering). Secondly, the depth distribution is influenced by the stopping power which increases with Z. Thirdly, the maximum transferable energy in a binary collision which is determined by $T = E_0 \cdot 4M_1M_2/(M_1+M_2)^2$ that depends on the mass ratio of projectile and target mass M_1 and M_2, respectively. The large difference between the different species plotted in Fig. 2 is mostly due to the different scattering cross sections. The in-

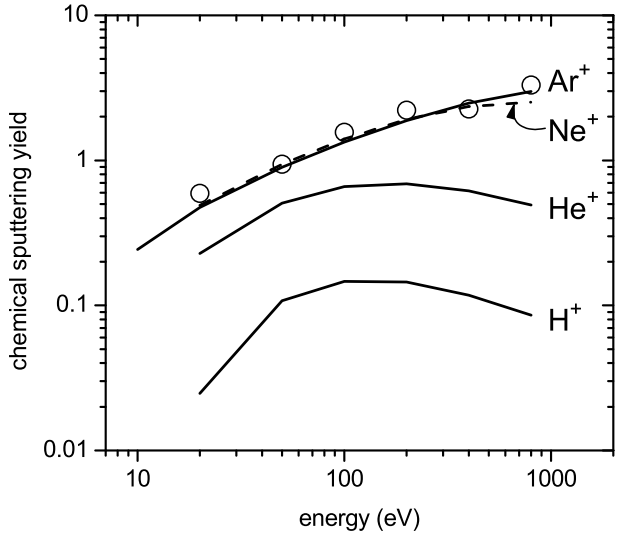

FIG. 3: Calculated chemical sputtering yields according to Eq. (1) assuming $a = 0.4$ (lines) for H^+, He^+, Ne^+, and Ar^+. The measured yields for Ar^+ (○) are shown for comparison.

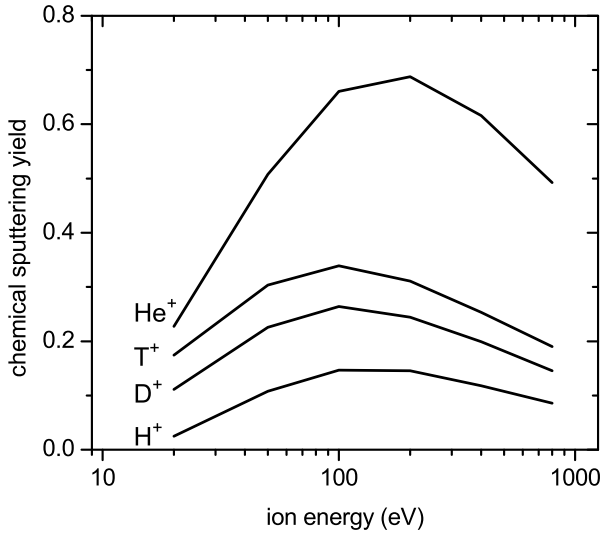

FIG. 4: Calculated chemical sputtering yields according to Eq. (1) ($a = 0.4$) for H^+, D^+, T^+, and He^+. The differences of the yields for H, D, and T are merely due to the differences of the maximum transferable energy which allow a larger energy transfer to carbon atoms with increasing projectile mass. The significant increase of the yield between T and He is due to the dependence of the nuclear scattering cross-section on the nuclear charge Z.

fluence of the maximum transferable energy can best be seen comparing the depth distributions for H, D, and T. Here the nuclear charge is identical, but the masses differ. With increasing mass it becomes easier to transfer energy to the carbon target atoms (T increases from hydrogen to tritium) and hence the displacement density increases.

Based on these depth distributions for the carbon displacement yield, the chemical sputtering yield for H^+, He^+, Ne^+, and Ar^+ ions is calculated. It is presented in Fig. 3 together with the measured data for Ar^+. For all cases a normalization factor $a = 0.4$ was used. As anticipated from the previous discussion, the chemical sputtering yield increases significantly with increasing nuclear charge of the ions. From H to Ar it increases by more than one order of magnitude. It is interesting to note that, according to these predictions, the yield for neon and argon is almost identical. Obviously, the higher stopping power and scattering cross section of argon are compensated by the higher maximum transferable energy in neon–carbon collisions ($T_{Ne} = 0.938E_0$, $T_{Ar} = 0.710E_0$).

In Fig. 4, the model results for the species most relevant for a fusion device, namely H^+, D^+, T^+, and He^+ are shown. With increasing mass of the projectile, the chemical sputtering yield increases. For H^+, D^+, and T^+ the maximum yield occurs around 100 eV. At this energy the calculated yields behave as 1 : 1.8 : 2.3. At lower energies the relative increase is even higher. The significant increase of the yield between T and He is due to the dependence of the nuclear scattering cross section on the nuclear charge Z. The isotope effect for H and D predicted by the model is well known in the literature. In ion-beam experiments, using H^+ and D^+ only (no additional atomic H), the yield due to D^+ impact is about a factor of 1.5 to 2 higher than that for H^+ [2, 14, 19–22]. Similar enhancement factors are found in plasma experiments where ions and atoms interact simultaneously with the surface [23, 24]. It is interesting to note that the much higher calculated chemical sputtering yield of Ne compared with D (compare Figs. 3 and 4) is in accord with the observation by Wampler *et al.* [25] that detachment by injection of neon in the DIII-D divertor leads to a much stronger carbon erosion as compared with deuterium. It is further obvious from Fig. 4 that the erosion of carbon due to chemical sputtering in a future nuclear fusion device using a D/T mixture will be higher than that measured in present machines using D/H mixtures as operating gas. The yield will increase further if helium or other extrinsic impurities will constitute a substantial contribution to the energetic particle flux to the surface.

D. New data for neon

Identical experiments as those presented in Fig. 1 for argon were performed using neon ions. The ion flux density for this experiment was between 3.8×10^{12} and $4.7 \times 10^{12}\,cm^{-2}\,s^{-1}$. The hydrogen atom flux density was $\sim 1.4 \times 10^{15}\,cm^{-2}\,s^{-1}$, so that the ratio of H to ion flux is about 350. The experiments were performed at a surface temperature of about 320 K. The results are shown in Fig. 5. As for argon, physical sputtering by neon ions alone is well described be TRIM.SP calculations. Thermally induced chemical erosion due to atomic hydrogen alone leads to an erosion rate of about 9×10^{11} carbon atoms $cm^{-2}\,s^{-1}$ (dashed line, right-hand scale). Simultaneous interaction of both species with the surface causes chemical sputtering with a yield being much higher than the sum of the yields of the individual species.

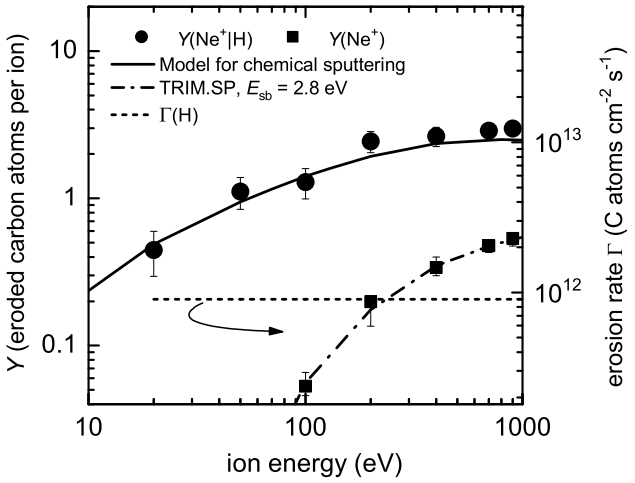

FIG. 5: Same as Fig. 1 but for neon ions (H atom flux density $\sim 1.4 \times 10^{15}\,\mathrm{cm^{-2}\,s^{-1}}$, atom-to-ion flux ratio ~ 350, $T = 320\,\mathrm{K}$).

The experimental data show an excellent agreement with the predictions of the chemical sputtering model (Eq. (1)) using the same normalization factor $a = 0.4$. This gives remarkable support to the model. As shown in Fig. 3, neon ions give rise to a very similar chemical sputtering yield as argon ions.

IV. SUMMARY

Chemical sputtering processes in the system hydrogen and carbon were studied in an UHV-based system working with well-defined, quantified particle beams. For the experiments presented in this paper, two species were used simultaneously: neutral atomic hydrogen and one species of low-energy ions (Ar^+ or Ne^+).

A microscopic model for chemical sputtering was discussed which is able to quantitatively reproduce the energy dependence of chemical sputtering by atomic hydrogen and arbitrary ions. The erosion yield of a specific ion is determined by the ability of this ion to break carbon–carbon bonds in the top surface layer of about 2 nm. This bond-breaking efficiency is determined by the mass and the nuclear charge of the projectile and can be computed with simulation codes such as TRIM.SP. The mass dependence of the bond-breaking efficiency is the reason for the observed isotope effect, i.e., a significantly higher yield for deuterium ions compared with protium ions. For excess supply of atomic hydrogen the chemical sputtering yield (eroded carbon atoms per incident ion) can reach very high values compared with simple physical sputtering. For example, the chemical sputtering yield using argon ions at 200 eV saturates around 3 ($j_\mathrm{H}/j_\mathrm{Ar} >$ several 100), while the measured physical sputtering yield is about 0.1. On the other hand, if we calculate the yield per impinging atomic hydrogen atom, the yield per H atom increases by a factor of 10 compared with simple thermally induced chemical erosion. This can be interpreted such that additional ion bombardment significantly enhances the reactivity of the surface towards reaction with atomic hydrogen. Model calculations for the chemical sputtering of carbon by atomic hydrogen and different ions relevant to plasma–wall interaction in nuclear fusion devices were presented.

[1] Federici, G., *et al.* Nucl. Fusion **41**, 1967 (2001).
[2] Vietzke, E., and Haasz, A. A., in *Physical Processes of the Interaction of Fusion Plasmas with Solids,* edited by W. Hofer and J. Roth (Academic Press, 1996), p. 135.
[3] Haasz, A. A., Mech, B. V., and Davis, J. D., J. Nucl. Mater. **231**, 170 (1996).
[4] David, J. W., Haasz, A. A., and Stangeby, P. C., J. Nucl. Mater. **155–157**, 234 (1988).
[5] Hopf, C., von Keudell, A., Jacob, W., Nucl. Fusion **42**, L27 (2002).
[6] Hopf, C., von Keudell, A., Jacob, W., J. Appl. Phys. **94**, 2373 (2003).
[7] Winters, H. F., and Coburn, J. W., Surf. Sci. Reports **14**, 161 (1992).
[8] Jacob, W., Hopf, C., von Keudell, A., Meier, M., and Schwarz-Selinger, T., Rev. Sci. Instrum. **74**, 5123 (2003).
[9] von Keudell, A., and Jacob, W., Prog. Surf. Sci. **76**, 21 (2004).
[10] Eckstein, W., *Computer simulation of ion-solid interactions* (Springer Series in Materials Science, Berlin and Heidelberg, 1991), 1st ed.
[11] Schlüter, M., Hopf, C., and Jacob, W., unpublished, 2005.
[12] Jacob, W., Hopf, C., and Schlüter, M., Appl. Phys. Lett. **86**, 204103 (2005).
[13] Eckstein, W., Sagara, A., and Kamada, K., J. Nucl. Mater. **150**, 266 (1987).
[14] Balden, M., and Roth, J., J. Nucl. Mater. **280**, 39 (2000).
[15] Hopf, C., and Jacob, W., A., J. Nucl. Mater. **342**, 141 (2005).
[16] Pillath, J., Winter, J., and Waelbroek, F., in *Amorphous hydrogenated carbon films,* edited by P. Koidl and P. Oelhafen (Les Éditions de Physique, 1987), E-MRS Symposia Proc., Vol. XVII, p. 449.
[17] von Keudell, A., and Jacob, W., J. Appl. Phys. **79**, 1092 (1996).
[18] Jacob, W., Thin Solid Films **326**, 1 (1998).
[19] Roth, J., and García-Rosales, C., Nucl. Fusion **36**, 1647 (1996); see also corrigendum: Roth, J., and García-Rosales, C., Nucl. Fusion **37**, 897 (1997).
[20] Roth, J., J. Nucl. Mater. **266–269**, 51 (1999).
[21] Mech, B. V., Haasz, A. A., and Davis, J. W., J. Appl. Phys. **84**, 1655 (1998).
[22] Mech, B. V., Haasz, A. A., and Davis, J. W., J. Nucl. Mater. **255**, 153 (1998)
[23] Jacob, W. Landkammer, B., and Wu, C., J. Nucl. Mater. **266–269**, 552 (1999).
[24] Fantz, U., and Paulin, H., Physica Scripta **T91**, 25 (2001).
[25] Wampler, W. R., Whyte, D. G., Wong, C. P. C., and West, W. P., J. Nucl. Mater. **313–316**, 333 (2003).